Inorg. Chem. **2007**, *46*, 7253–7255

Phenylimido Functionalization of α-$[PW_{12}O_{40}]^{3-}$

Jeff C. Duhacek and Dean C. Duncan*

Department of Chemistry and Biochemistry, University of Wisconsin—Milwaukee, Milwaukee, Wisconsin 53201

Received May 25, 2007

A synthetic route of potentially wide scope is reported herein for the organoimido functionalization of polyoxotungstates. This report focuses on the reaction between the monovacant lacunary polyoxotungstate, α-$((n\text{-}C_4H_9)_4N)_4H_3[PW_{11}O_{39}]$, and $W(NC_6H_5)Cl_4$ in anhydrous acetonitrile. Evidence from ^1H, ^{31}P, ^{183}W, and ^1H–^{183}W HMQC NMR spectroscopy, as well as cyclic voltammetry, electronic absorption, and elemental analysis, is presented for the formation of α-$[PW_{12}O_{39}(NC_6H_5)]^{3-}$ (**2**) of C_s symmetry, which is structurally related to T_d α-$[PW_{12}O_{40}]^{3-}$ (**3**) by formal oxide substitution. The electronic structure of **2** is significantly perturbed from **3** with significant arylimido → tungsten charge transfer, primarily localized to the $W(NC_6H_5)$ fragment with secondary charge delocalization onto the remaining W and corner-shared bridging O atoms. This is consistent with the ∼800 ppm downfield ^{183}W NMR shift for the phenylimido–tungsten, modest cathodic shifts in reversible redox potentials, electronic and IR spectra, and density functional theory calculations.

The first organic derivatives of polyoxometalates (POMs) were reported independently in 1978−1979 by Ho and Klemperer[1a] for α-$[PW_{11}O_{39}(TiC_5H_5)]^{4-}$, and Knoth and coworkers[1b,c] and Zonnevijlle and Pope[1d] for α-$[PW_{11}O_{39}(MR)]^{4-}$ (MR = organogermanium, tin, and lead). Since then, considerable efforts have been directed toward the organic functionalization of redox-active closed-framework POMs, particularly the molecular metal oxide anions of Mo and W in their formal d^0 oxidation states.[2] Our motivations for functionalizing POM surfaces include the following: (1) access to structurally well-defined complexes for investigating structure/property relationships emerging at the interface between organic species and catalytically active metal oxide surfaces; (2) in a related point, the tuning of POM properties, particularly redox, photoredox, and photoaction spectra to include visible light, a necessary condition for developing POM-based photocatalysts that harness solar energy; (3) the supramolecular construction of redox-active POMs via both self-assembly and covalent tethering of the organic components into functional POM-based materials.

A promising approach toward the surface functionalization of closed-framework POMs involves the formal substitution of terminal oxo ligands for nitrido or organoimido ligands. The groups of Errington, Maatta, and Peng independently established oxo metathesis routes to the organoimido functionalization of hexamolybdate, $[Mo_6O_{19}]^{2-}$, and also prepared redox-active oligomers and polymers from monomeric $[Mo_6O_{19-x}(NR)_x]^{2-}$ units.[3,4a−c] Recently, Wei reported access to alkenyldiimido-bridged hexamolbydate dimers via dehydrogenative coupling of primary amines with α-$[Mo_8O_{26}]^{4-}$.[4d] However, an oxo metathesis approach does not appear to extend to POMs other than hexamolybdate, and therefore new routes of broader scope for POM functionalization are needed. This is particularly true for the polyoxotungstates because these anions are expected to be both more stable and inert than isostructural polyoxomolybdates as a result of the greater inherent strength of W−O bonds. Unfortunately, it is this feature that also renders polyoxotungstates unreactive to oxo metathesis. Indeed, only a single example of a functionalized isopolyoxotungstate exists, namely, $[W_6O_{18}(NC_6H_5)]^{2-}$, which is prepared in ∼8% yield from mononuclear precursors yet demonstrates superior thermal and hydrolytic stability relative to $[Mo_6O_{18}(NC_6H_5)]^{2-}$.[5a]

A different synthetic approach is illustrated below for the organoimido substitution of an α-Keggin anion. It involves

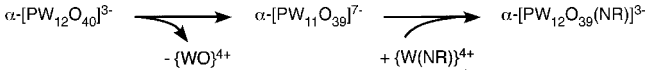

* To whom correspondence should be addressed. E-mail: dcduncan@uwm.edu.

(1) (a) Ho, R.; Klemperer, W. *J. Am. Chem. Soc.* **1978**, *100*, 6772. (b) Knoth, W.; Domaille, P.; Roe, D. *Inorg. Chem.* **1983**, *22*, 198. (c) Knoth, W.; Harlow, R. *J. Am. Chem. Soc.* **1981**, *103*, 4265. (d) Zonnevijlle, F.; Pope, M. *J. Am. Chem. Soc.* **1979**, *101*, 2731.

(2) Reviews: (a) Gouzerh, P.; Proust, A. *Chem. Rev.* **1998**, *98*, 77. (b) Pope, M., Müller, A., Eds. *Polyoxometalate Chemistry: From Topology via Self-Assembly to Applications*; Kluwer: Dordrecht, The Netherlands, 2001.

(3) (a) Clegg, W.; Errington, J.; Fraser, K.; Holmes, S.; Schäfer, A. *Chem. Commun.* **1995**, 455. (b) Du, Y.; Rheingold, A.; Maatta, E. *J. Am. Chem. Soc.* **1992**, *114*, 345. (c) Strong, J.; Yap, G.; Ostrander, R.; Liable-Sands, L.; Rheingold, A.; Thouvenot, R.; Gouzerh, P.; Maatta, E. *J. Am. Chem. Soc.* **2000**, *122*, 639. (d) Moore, A.; Kwen, H.; Beatty, A.; Maatta, E. *Chem. Commun.* **2000**, 1793.

(4) (a) Wei, Y.; Xu, B.; Barnes, C.; Peng, Z. *J. Am. Chem. Soc.* **2001**, *123*, 4083. (b) Xu, B.; Lu, M.; Kang, J.; Wang, D.; Brown, J.; Peng, Z. *Chem. Mater.* **2005**, *17*, 2841. (c) Lu, M.; Xie, B.; Kang, J.; Chen, F.; Yang, Y.; Peng, Z. *Chem. Mater.* **2005**, *17*, 402. (d) Li, Q.; Wei, Y.; Hao, J.; Zhu, Y.; Wang, L. *J. Am. Chem. Soc.* **2007**, *129*, 5810.

10.1021/ic701024c CCC: $37.00
Published on Web 08/02/2007

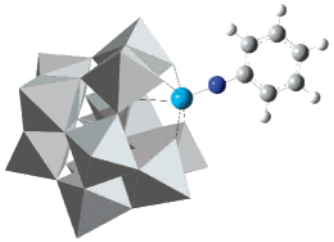

Figure 1. Polyhedral representation of **2**.

the hydrolytic removal of a formal $[WO]^{4+}$ fragment from the POM surface to form a lacunary or monovacant POM wherein the closed structure is then reformed in a second step by insertion of a formal $[M(NR)]^{n+}$ unit via the addition of suitably reactive reagents. This approach was first reported in nonaqueous media by Klemperer and co-workers, who isolated $[PW_{11}O_{39}(TiC_5H_5)]^{4-}$ as a tetra-*n*-butylammonium (Q^+) salt from the reaction between α-$Q_4H_3[PW_{11}O_{39}]$ (Q_4H_3**1**) and $(C_5H_5)TiCl_3$ in anhydrous organic solvents.[1a] This was extended more recently by Proust for the preparation of organoimido α-$[PW_{11}O_{39}(Re^{V}(NC_6H_5))]^{4-}$, as well as Proust and Maatta for the nitrido complexes α-$[PW_{11}O_{39}(Re^{VI}N)]^{4-}$ and α-$[PW_{11}O_{39}(Os^{VI}N)]^{4-}$, by reaction of Q_4H_3**1** with $Re(NC_6H_5)(PPh_3)_2Cl_3$, $ReNCl_2(PPh_3)_2$], and $[OsNCl_4]^-$, respectively.[5b,c] Extending this approach further, we report herein the first synthesis of an organoimido-functionalized iso-addenda heteropolyoxotungstate, α-$[PW_{12}O_{39}(NC_6H_5)]^{3-}$ (**2**), where the metal framework "addenda" consist entirely of W atoms (Figure 1).[6]

The addition of $W(NC_6H_5)Cl_4$[7] (1 equiv) to a stirred anhydrous acetonitrile solution containing Q_4H_3**1** (200 mg, 1 equiv) and triethylamine (3 equiv) under a dry N_2 atmosphere at 25 °C results in the rapid formation (<20 min) of both **2** and α-$[PW_{12}O_{40}]^{3-}$ (**3**) as identified by ^{1}H and ^{31}P NMR spectral monitoring of the reaction mixture. A yellow-brown air-stable microcrystalline solid is isolated in 93% yield based on Q_4H_3**1** and is formulated as a mixed Q^+ salt of both anions, **2** and **3**.[8] The purity of **2** in this material varies between 67 and 94% and is identical with that of the initial reaction mixture solution. Surprisingly, attempts to purify this solid by recrystallization from numerous solvent systems, solid-phase extraction, or reversed-phase chromatography all fail to separate the two isocharged anions because there is no change in the measured product purity, even though the samples are highly crystalline (usually thin plates) and appear to be homogeneous in color and crystal

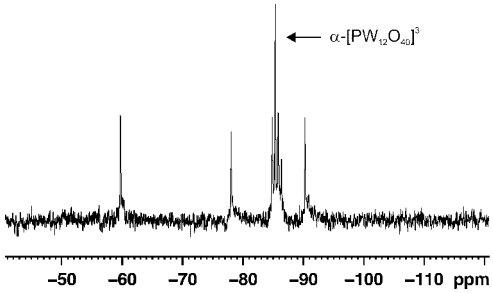

Figure 2. ^{183}W NMR (20.8 MHz) spectrum of **2** in DMF-d_7 (250 mg in 500 μL; 15 360 scans). The CPMG pulse sequence (echo time = 1.5 ms) was used to eliminate acoustic ringing and pulse breakthrough artifacts. Chemical shifts are reported relative to 2 M $Na_2[WO_4]$ in D_2O.

morphology. This behavior has precedence because the Q^+ salts of α-$[PW_{11}O_{39}(Re^{V}(NC_6H_5))]^{4-}$ and α-$[PW_{11}O_{39}(Re^{V}O)]^{4-}$ also could not be separated.[5c] In fact, this behavior appears to be symptomatic of arylimido-substituted α-Keggin complexes in general because the series of aryl-substituted derivatives of **2** mentioned earlier all exhibit the same problem of purification, despite large differences in electronic and steric properties of the appended substituents. This suggests that the polyanion lattice packing energetics, while being clearly dominated by long-range Coulombic interactions, are influenced very little by the presence of the aryl ring. This, in turn, is likely related to a 12-fold positional disorder of the arylimido substituent in the unit cell[5c] and is consistent with our inability to obtain full structure solutions from X-ray diffraction data collected on single crystals of different arylimido Q^+ salt derivatives. Similar difficulties are reported in structural investigations of transition-metal-substituted Keggin and other derivatives.[1a,5b,c]

The ^{31}P, ^{1}H, and ^{183}W NMR and IR spectra are consistent with the proposed C_s-symmetry structure for **2**. The triply degenerate P−O asymmetric stretch of **3** (1080 cm^{-1}) splits into two IR absorption bands in **2** (1080 and 1066 cm^{-1}; KBr) with bathochromic shifts of 2−5 cm^{-1} for the remaining three principal, and unsplit, bands of the Keggin framework. Similar behavior is observed in metal-substituted α-Keggin C_s-symmetry complexes.[1a,5b,c] In CD_3CN, **2** exhibits a single ^{31}P NMR resonance at −14.05 ppm versus 85% H_3PO_4, whereas the same peak for **3** resonates downfield at −13.80 ppm (Figure S1 in the Supporting Information). The ^{1}H NMR spectrum of **2** in CD_3CN consists of three sets of aromatic ^{1}H NMR resonances: δ 7.65 (t, 2H, meta), 7.20 (t, 1H, para), and 7.18 (d, 2H, ortho). The integrations of these resonances relative to those of the Q^+ counterions accurately reflect the extent of contamination by **3**, as judged independently by ^{31}P NMR.

The ^{183}W NMR spectrum of **2** in dimethylformamide-d_7 (DMF-d_7) shows six peaks clustered between −50 and −100 ppm relative to 2 M Na_2WO_4/D_2O in a 2:2:2:2:1:2 relative ratio as well as a single resonance at −85.3 ppm assigned to **3** by comparison with an authentic sample (Figure 2). This spectrum is consistent with the proposed C_s symmetry of **2**, where the ^{183}W NMR resonances are assigned to the 11 W atoms bearing terminal oxo ligands. The unique tungsten coordinated to the phenylimido ligand is not observed in a simple 1-D experiment presumably because of T_2 broadening

(5) (a) Mohs, T.; Yap, G.; Rheingold, A.; Maatta, E. *Inorg. Chem.* **1995**, *34*, 9. (b) Kwen, H.; Tomlinson, S.; Maatta, E.; Dablemont, C.; Thouvenot, R.; Proust, A.; Gouzerh, P. *Chem. Commun.* **2002**, 2970. (c) Dablemont, C.; Proust, A.; Thouvenot, R.; Afonso, C.; Fournier, F.; Tabet, J.-C. *Inorg. Chem.* **2004**, *43*, 3514.

(6) We also have prepared several other aryl ring-substituted derivatives, which will appear in a future report.

(7) Pedersen, S.; Schrock, R. *J. Am. Chem. Soc.* **1982**, *104*, 7483.

(8) Anal. Calcd for $C_{48+6x}H_{108+5x}N_{3+x}PW_{12}O_{40-x}$ (x = 0.94): C, 17.53; H, 3.09; N, 1.50. Found: C, 17.65; H, 3.09; N, 1.49. IR (KBr, 400−1200 cm^{-1}): P−O 1080 (s), 1066 (m), W=O 975 (s), W−O−W 894 (s), 811 (vs) cm^{-1}. UV−vis (CH_3CN, 300−900 nm): λ_{sh} 312 and 475 nm. ^{1}H NMR (CD_3CN, Me_4Si = 0, 500 MHz): δ 7.65 (t, 2H, meta), 7.20 (t, 1H, para), 7.18 (d, 2H, ortho). ^{31}P NMR (CD_3CN, H_3PO_4 = 0, 202 MHz): δ −14.05. ^{183}W NMR (DMF-d_7, Na_2WO_4 = 0, 20.8 MHz): δ −59.8 (2), −78.0 (2), −84.9 (2), −85.9 (2), −86.4 (1), −90.3 (2); +745 (1; detectable only by ^{183}W−^{1}H HMQC).

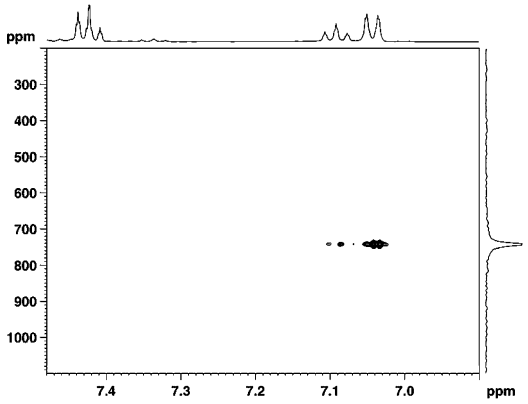

Figure 3. $^{183}W-^{1}H$ HMQC NMR (20.8 MHz, 500 MHz) spectrum of **2** in DMF-d_7 (250 mg in 500 μL).

Table 1. Selected Bond Lengths and Charges from Geometry-Optimized Structures of **2** and **3**[a]

bond	bond length (pm)[b]	moiety	Mulliken pop.[c]
W−N	177.6 (**2**)	W_N; C_6H_5N	1.998 (**2**); −0.492 (**2**)
W−O_t	172.7 (**2**);[d] 172.5 (**3**)	W_O	2.085 (**2**);[d] 2.088 (**3**)
W_N−OP	240.2 (**2**)	$O_{b,c}$	−0.796 (**2**);[d] −0.794 (**3**)
		$O_{b,e}$	−0.784 (**2**);[d] −0.784 (**3**)
W_O-OP	246.0 (**2**);[d] 245.1 (**3**)	O_t	−0.623 (**2**);[d] −0.623 (**3**)

[a] ADF2006.01 program. Triple-ζ ZORA relativistic basis sets with two polarization functions on all atoms except H (W frozen core 1s−4spdf). [b] SVWN5 (LDA) functional. [c] SVWN5 (LDA) + BP86 (GGA). [d] Averaged over all such units in the structure. W_N = phenylimido−tungsten; W_O = all other tungstens; O_t = terminal oxo; O_b = μ_2-bridging oxygen (c, corner; e, edge).

arising from the adjacent quadrupolar ^{14}N nucleus; however, it is detected in a $^{1}H-^{183}W$ HMQC experiment as a single broad ^{183}W peak at +745 ppm, which cross-correlates with the *o*- and *p*-H atoms of the phenyl ring (Figure 3). Similar cross-correlations for long-range $^{4}J_{H-W}$ and $^{6}J_{H-W}$ couplings have been reported for mononuclear arylimido−tungsten complexes.[9]

The anticipated thermal and hydrolytic stabilities of **2** are confirmed in an acetonitrile solution. In the presence of either water (10 equiv) under reflux for 3 days or HBr (3 equiv) under ambient conditions, no decomposition is detected by ^{1}H or ^{31}P NMR, suggesting that the formation of **3** during the synthesis of **2** likely occurs via a concurrent pathway.

In the absence of direct structural information, density functional theory (DFT) calculations can provide insight on the structural and electronic perturbations of the Keggin framework induced by the phenylimido ligand (Table 1).[10] The principal differences between the optimized geometries of **2** and **3** are reminiscent of those between structurally characterized $[M_6O_{18}(NC_6H_5)]^{2-}$ and $[M_6O_{19}]^{2-}$ (M = Mo^{6+} and W^{6+}), which also have been modeled successfully using DFT methods.[3−5a,11] These include (1) a linear W−N−C bond angle (179.9°) consistent with multiorbital (σ and π) W−N bonding, (2) shorter terminal W−O versus W−N bonds, (3) and longer (PO)−W bonds when trans to terminal W−O versus W−N. Relative differences between the atom charge values obtained from Mulliken populations both within **2** and between **2** and **3** offer qualitative insight into the influence of the phenylimido ligand on the POM charge distribution. The results show increased charge transfer to the POM framework upon phenylimido substitution (Δ = −0.131*e*), as is expected from the greater π-donor ability and lower electronegativity of the phenylimido versus oxo ligand.[12] An additional −0.006*e* of charge is transferred from the central PO_4^{3-} to the $W_{12}O_{35}(NC_6H_5)$ framework. The excess charge in **2** is localized primarily on the unique phenylimido−tungsten atom (66%) with residual charge delocalized onto the other W atoms (19%) and the corner-shared bridging O atoms (14%). Little charge accumulates on the edge-shared bridging and terminal O atoms. Predominant localization of the phenylimido → tungsten charge transfer is reflected further in the Kohn−Sham molecular orbitals and ^{183}W NMR chemical shifts. The highest occupied molecular orbital (HOMO) in **2** is predominantly aryl C−C and W d−N p π bonding in character with no contributions from other W atoms, whereas in **3**, the HOMO is nonbonding with bridging O p character, O_b p.[13a] The increased paramagnetic contribution in the ∼800 ppm downfield ^{183}W NMR chemical shift of the phenylimido versus terminal oxo W atoms also is consistent with increased "d-orbital" electron occupancy, wherein the absence of similarly large chemical shift changes for the other ^{183}W NMR resonances in **2** further reflects the localized nature of this charge transfer. Magnetic-field-induced mixing of low-lying excited states into the ground state may also contribute to the increased paramagnetic contribution because the electronic spectrum of **2** confirms new transitions in the visible region that are absent in **3**. The secondary delocalization of charge transferred from the $W(NC_6H_5)^{4+}$ fragment across multiple W atoms is reflected in the redox potentials of **2**, wherein the lowest unoccupied molecular orbital (LUMO) is tungsten-centered with multiple W $d_{xy}-O_b$ p slightly antibonding π^* contributions. The cyclic voltammogram of **2** in acetonitrile (1 mM **2** in a 0.1 M $Q^+[PF_6]^-$ electrolyte versus 0.01 M $Ag/AgNO_3$) consists of three quasireversible monoelectronic half-wave potentials at −0.704, −1.211, and −1.894 V that are similar to **3** but are cathodically shifted by −119, −99, and −74 mV, respectively. The first electron affinity difference (ΔEA) between **2** and **3** is approximated by their relative LUMO energies.[13b] Accounting for solvation within the conductor-like screening model (COSMO), the estimated ΔEA is −102 meV, in reasonable agreement with experiment (−119 mV).

Acknowledgment. We thank F. Holger Försterling for assistance with the HMQC experiment. The University of Wisconsin System is gratefully acknowledged for support.

Supporting Information Available: Synthesis of **2** and the ^{31}P NMR spectrum of the mixture of **2** and **3**. This material is available free of charge via the Internet at http://pubs.acs.org.

IC701024C

(9) Macchioni, A.; Pregosin, P.; Rüegger, H.; van Koten, G.; van der Schaaf, P.; Abbenhuis, R. *Magn. Reson. Chem.* **1994**, *32*, 235.
(10) Further details on the results of these and related calculations will be published separately.
(11) Yang, G.; Guan, W.; Yan, L.; Su, Z.; Xu, L.; Wang, E. *J. Phys. Chem. B* **2006**, *110*, 23092.
(12) Nugent, W.; Mayer, J. *Metal−Ligand Multiple Bonds*; Wiley-VCH: New York, 1988.
(13) (a) Maestre, J.; Lopez, X.; Bo, C.; Poblet, J.; Casan-Pastor, N. *J. Am. Chem. Soc.* **2001**, *123*, 3749. (b) Lopez, Z.; Fernandez, J.; Poblet, J. *Dalton Trans.* **2006**, 1162.